Journal of Multidisciplinary Engineering Science and Technology (JMEST)
ISSN: 2458-9403
Vol. 5 Issue 11, November - 2018

Detection of Buried Pipelines Transporting Hot Fluids using Infrared Thermography

Jonas Kavi[1], **Udaya B. Halabe**[1]
[1] Constructed Facilities Center, Department of Civil and Environmental Engineering
West Virginia University
Morgantown, WV, USA.
Jokavi@mix.wvu.edu; Udaya.Halabe@mail.wvu.edu

***Abstract*— Detection of buried utilities such as pipelines is essential for infrastructure asset management operations. Pipeline locating operations are carried out during construction, rehabilitation, or farming activities in order to avoid digging into the buried pipeline; or to locate the pipe for maintenance work. Several techniques exist for locating buried pipelines, including Ground Penetrating Radar (GPR) and tracer wires. GPR is less effective in locating non-metallic pipes or pipes buried in very wet and electrically conductive soils, while the tracer wire technique can only be used if the wires are buried with the pipe. A method of locating buried pipelines transporting hot fluids using Infrared Thermography (IRT) is presented in this paper. Additionally, IR cameras come in portable and compact form factors, which make it possible for it to be mounted on UAVs (Unmanned Aerial Vehicles) or to be integrated into UAV inspection systems. A 7.6 cm (3 inch) diameter Carbon Fiber Reinforced Polymer (CFRP) composite pipe buried at 35.6 cm (14 inch) depth and transporting hot water was easily detected in the laboratory using IRT. A 15.2 cm (6 inch) diameter pipe buried at 91.4 cm (3 ft) depth and transporting steam in the field environment was also detected all year round in different weather conditions with IRT. The laboratory and field results offer a great potential for detecting pipelines transporting hot petroleum from production wells and refineries, as well as pipes transporting fluids with significantly higher or lower temperatures with respective to the surrounding soil.**

Keywords—Infrared thermography (IRT); FRP; composite; buried pipe detection

I. INTRODUCTION

Infrared thermography (IRT) is one of the widely used nondestructive testing techniques for infrastructure monitoring. It has been employed in various monitoring operations such as fatigue crack detection, quality evaluations of bonded Fiber Reinforced Polymer (FRP) strengthening systems, insulation quality inspection, and bridge deck inspections [1-8]. IRT operates on the principle of heat transfer from hotter to colder regions within an object. Object and feature detection using this technique is based on the variation of electromagnetic radiations reflected or emitted by the object of interest and its surroundings. Different materials have different thermal characteristics, and this affects the rate of energy flow through and from the material. An infrared sensor/camera is used to measure the variations in energy emitted from an object, which is converted into a thermographic image, representing thermal characteristics of the object. Most infrastructure applications of IRT (such as bridge deck monitoring and testing fiber reinforced polymer wraps) rely on solar heating of the object of interest. In cases where solar heating is insufficient or unavailable, other active heat source is required.

Though there is not much literature on the use of IRT for buried pipe detection, it is anticipated that the technique can be applied in detecting buried pipelines transporting hot fluids. Thus, the feasibility of detecting subsurface pipelines transporting hot fluid using IRT was explored in this research. Since petroleum products are hot in the initial part of the pipeline (within about 5 miles from the source of production wells), the IRT technique offers some promise for detecting such pipeline sections. Furthermore, there is the potential for detecting pipelines carrying other hot fluids such as hot water or steam.

Other pipelines not transporting hot fluids may also be detected if their content has significant difference in thermal properties relative to the surrounding soil, and there is enough solar heating to produce a radiation contrast (limited to very shallow depths). An advantage of IRT is that, it is a non-contact technique, hence direct access to the pipeline is not required for detection and mapping. In addition, IR cameras also come in portable form factors, which offer a great potential for it to be mounted on UAVs (Unmanned Aerial Vehicles) or to be integrated into UAV inspection systems. This paper presents laboratory tests and results, in addition to field application of IRT for buried pipe detection.

II. IRT TEST EQUIPMENT

This study used InfraCAM SD thermal imager (Fig. 1a) manufactured by FLIR Systems, Inc. for the IRT testing. This is a portable handheld infrared camera with a spectral range of 7.5 to 13μm, a 0.12°C thermal sensitivity at 25°C, and ±2°C accuracy.

The type-T thermocouple probe (Fig. 1b) was used for contact temperature measurements. A 2.5x5 cm (1"x2") high temperature self-adhesive tape was used

The authors gratefully acknowledge the financial support provided by the USDOT-PHMSA through Project # DTPH5615HCAP09.

to attach the thermocouple to the pipe surface during testing. The thermocouple had a temperature range of -200°C to +260°C and a ±1.0°C accuracy for readings above 0°C. The thermocouples were read using an automated reader/recorder (Fig. 2a) that was built to enable continuous collection of temperature data on the buried pipe throughout the IRT testing period. Ambient temperature during the test was record using Thermo Recorder TR-72Ui (Fig. 2b).

(a) FLIR InfraCAM SD camera *(b) Type-T thermocouple (Source: Novatech USA)*

Fig. 1. *FLIR InfraCAM SD camera and type-T thermocouple*

III. Experimental Set-Up for IRT Testing

An insulated wooden box with an internal dimension of 61x61x30.5 cm (24"x24"x22" after insulation) was built for the IRT testing of buried Carbon Fiber Reinforced Polymer (CFRP) composite pipe carrying hot liquid. The insulation in the box (with R Value of 10) would ensure that heat detection (if any) will only be as a result of heat propagation from the hot pipe through the soil to the soil surface. Also, the insulation ensures no heat leakage out of the box, which will help in heat transfer computations to extrapolate the surface temperature for different soil depths. Fig. 3 and Fig. 4 show the wooden box and capped 7.6 cm (3") diameter CFRP pipe respectively. The CFRP pipe, fitted with aluminum caps was buried in the insulated box with hot water circulated through the pipe.

The pipe was buried in the box filled with a mixture of gravel, sand, and organic soil in the ratio of 1:1:2, and having a moisture content of 14%. 7.6 cm (3") depth of the soil mixture was placed at the bottom of the insulated box before the pipe was inserted. Soil cover above the pipe was 35.6 cm (14"), and 5 cm (2") space was left at the top of the box as shown in Fig. 5. The box was left open at the top during the experiments to simulate field conditions where the soil surface is exposed.

Five thermocouples were installed on the surface of the CFRP pipe before burying (3 thermocouples at the top and 2 at the bottom surface of the pipe as shown in Fig. 4). Another thermocouple was placed at the surface of soil in the box to measure soil surface temperature. The 6 thermocouples were connected to the automated recorder to enable continuous data collection. Hot water (at a temperature of 95°C) was circulated through the buried pipe, while the temperature changes at the surface of the buried pipe and the soil surface were recorded over a period of 10 days. Soil surface temperature was also recorded using infrared thermography (IRT) throughout the testing period. It should be noted that, water circulation was started with the water initially at room temperature (21.6°C), and it took 3 hours for the water temperature to rise to the 95°C level. Also, the hot water did not fully fill the pipe to the top due to entrapped air pocket. Hence top portion of the pipe was at 85.5°C and colder than the bottom portion by about 4.5°C because of the trapped air. The IRT test setup is shown in Fig. 5.

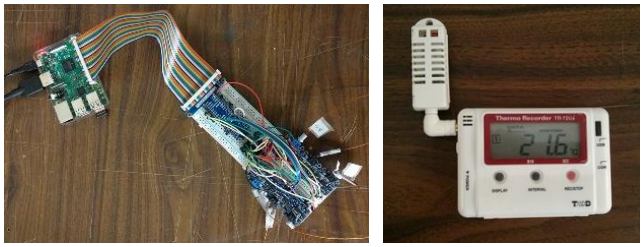

(a) (b)

Fig. 2. *(a) Automated thermocouple reader, (b) Thermo Recorder*

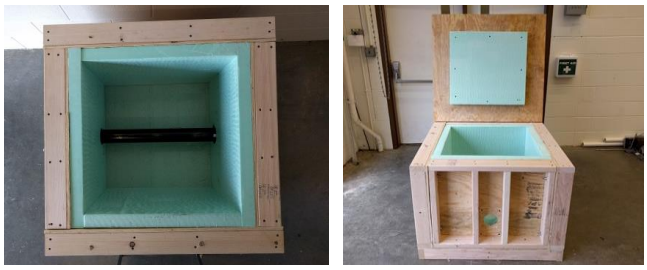

(a) (b)

Fig. 3. *Insulated wooden box used for IRT testing*

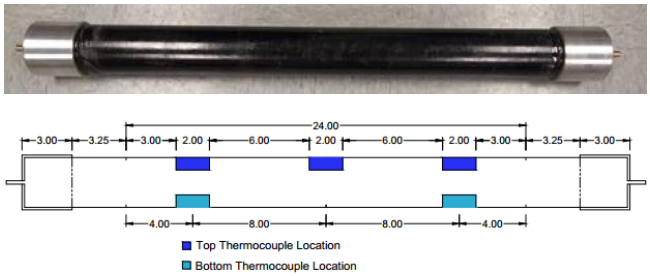

Fig. 4. *CFRP pipe for IRT testing (top), sketch showing thermocouple locations (bottom)*

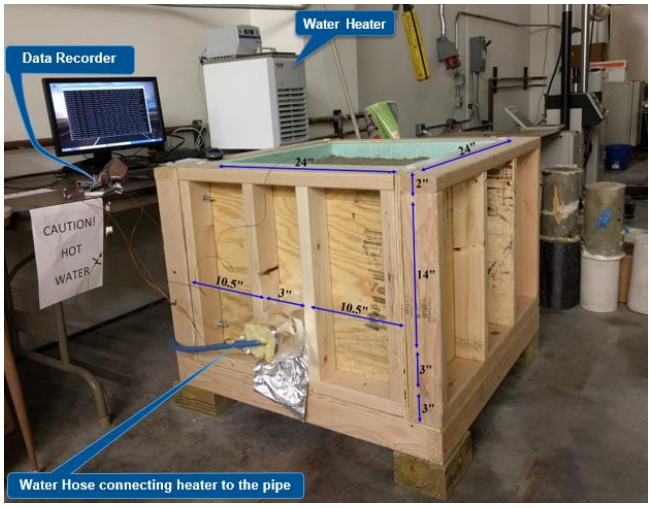

Fig. 5. *IRT test set-up*

IV. IRT Test Results

IRT testing was carried out to illustrate both the period when the pipeline is in operation and transporting hot fluids, and the period immediately following pipeline shut down or ceasing of pumping operations. Results from both testing phases are presented below.

A. Pipe Operating /Heating Cycle

As stated previously, the IRT test was carried out over a period of 10 days where hot water at a temperature of 95°C was circulated through the buried 7.6 cm (3") CFRP pipe. The temperature at the pipe and soil surfaces, and room/ambient temperatures were recorded over the testing period. Temperature at the soil surface had a sharper increase during the first 48 hours of testing, followed by a gradual increase up to the sixth day of testing. There was not much temperature increase between the sixth and tenth days of testing. Fig. 6 shows some of the IRT data at various stages of testing. Fig. 7 and Fig. 8 show plots of temperature changes during the test period. Each test day started at 8:00 am and ended at 7:59 am the following day. The small fluctuations (jitter) in temperatures shown in Fig. 7 and Fig. 8 are due to diurnal temperature changes between day and night. These diurnal changes are present in the laboratory data since the laboratory temperature was not regulated. Maximum daily temperatures recorded during the test occurred between 3:00 pm and 5:15 pm. The results (IRT curve in Fig. 7) show approximately 14°C increase in surface temperature of the soil for this pipe carrying hot liquid, thus making it possible to detect such buried pipes using infrared thermography measurements at the soil surface. Infrared thermography readings at the soil surface were found to be about 2-3°C higher than the thermocouple readings at the same location. The difference in surface temperature readings can be attributed to the accuracies of the infrared camera and the thermocouple, which are ±2°C and ±1.0°C respectively.

The following nomenclature are adoped to explain the IRT data in Fig. 6 through Fig. 8:

IRT: Infrared thermography image/data temperature reading at soil surface

TSC: Thermocouple reading taken at the center of the soil surface

Amb: Ambient/room temperature

TSC-Amb: Difference between TSC and Amb

IRT-Amb: Difference between IRT and Amb

The results show that, the 7.6 cm (3") diameter CFRP pipe buried with 35.6 cm (14") of soil cover and carrying 95°C of liquid can be detected at the ground surface using infrared thermography.

The experimental results were extrapolated using a one-dimensional heat transfer (conduction) formulation to estimate the depth at which the pipe will no longer be detectable using IRT. The heat transfer equation for one-dimensional heat conduction is given by (1).

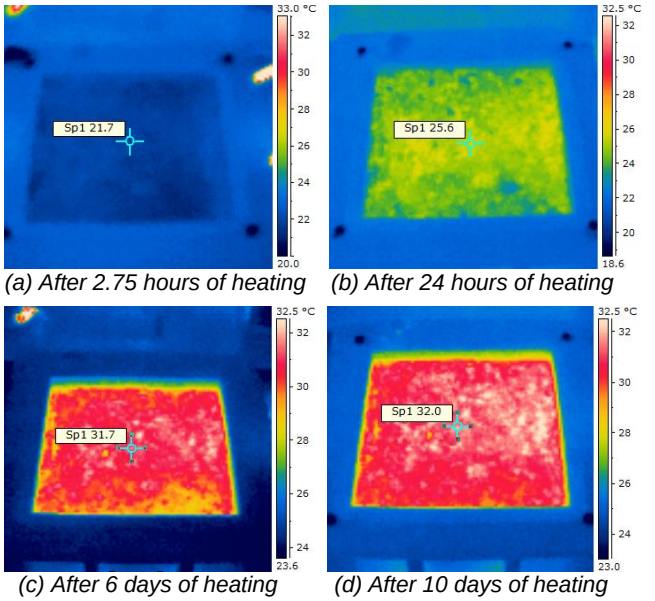

(a) After 2.75 hours of heating (b) After 24 hours of heating

(c) After 6 days of heating (d) After 10 days of heating

Fig. 6. *Infrared thermography data at the soil surface at various stages of testing*

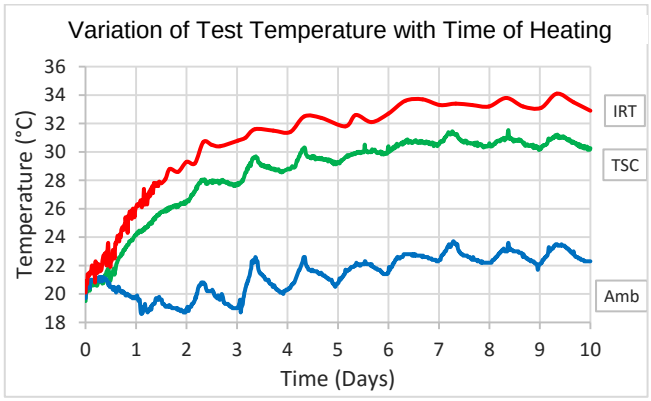

Fig. 7. *Variation of soil surface (TSC, IRT) and room (Amb) temperatures with time*

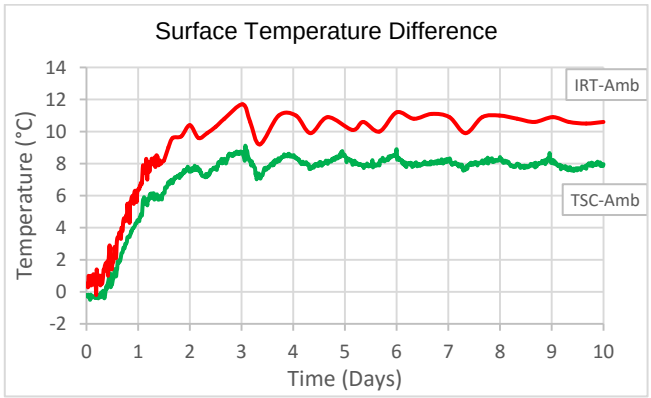

Fig. 8. *Soil surface temperature difference with time*

$$q_{net} = \frac{k}{d}(T_h - T_c) \quad (1)$$

where,

q_{net} = net heat flow through a unit area of a material per unit time (W/m^2)

k = thermal conductivity of the medium (W/m/°C)

T_h = temperature of the hotter side (°C)
T_c = temperature of the colder side (°C)
d = thickness/depth of the medium (m)

$$q_{net} = \frac{k}{d}(\Delta T) \quad (2)$$

$$\Delta T = T_h - T_c$$

$$\Delta T = \frac{q_{net}}{k}(d) \quad (3)$$

Assuming q_{net}/k is constant, that is:

$$\frac{q_{net}}{k} = \frac{\Delta T}{d} = constant \quad (4)$$

Thus given the same soil material with varying depths d_1 and d_2,

$$\Delta T_1 = \frac{q_{net}}{k}(d_1) \rightarrow \frac{q_{net}}{k} = \frac{\Delta T_1}{d_1}$$

$$\Delta T_2 = \frac{q_{net}}{k}(d_2) \rightarrow \frac{q_{net}}{k} = \frac{\Delta T_2}{d_2}$$

$$\frac{\Delta T_1}{d_1} = \frac{\Delta T_2}{d_2} \rightarrow \Delta T_2 = \frac{d_2 . \Delta T_1}{d_1} \quad (5)$$

Thus, using d_1 and ΔT_1 from the experiment, ΔT_i can be estimated for any given depth, d_i, of soil cover over a buried pipe if thermal properties of the soil are the same as used in the experiment. The ratio q_{net}/k was assumed to be constant for the soil mixture during the computation. The experimental data at day 6 was used as a baseline for this computation because the system had reached a steady state by that time as illustrated by the almost constant temperature difference in Fig. 8. All temperatures in this computation are from thermocouples readings:

q_{net}/k = $\Delta T/d$ = $\Delta T_1/d_1$, assumed constant (and computed using the following data)
T_h = Temperature at the surface of the buried pipe at day 6, measured to be 85.47°C
T_c = Temperature at the surface of the soil at day 6, measured to be 30.40°C (TSC)
d = depth of soil cover over the pipe, 35.6 cm (14")

Soil surface temperature differences (difference between soil surface temperature and room temperature or TSC-Amb) for different depths of soil cover were computed using (5). Sample computation results are shown in Table 1, and the results are plotted in Fig. 9. Table 1 and Fig. 9 also show the projected temperature difference using IRT (IRT-Amb), which is higher than TSC-Amb by 2.5°C at each data point. The plot in Fig. 9 shows that, the same 3" CFRP pipe buried in the same soil medium and carrying a liquid at 95°C will be detectable using IRT, up to a depth of about 42 cm (16.5"); with a temperature increase of about 1.6°C.

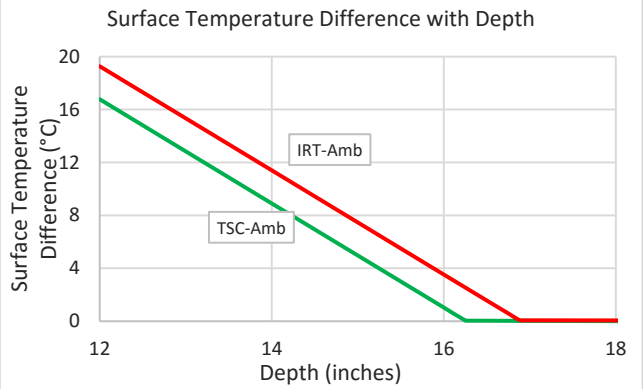

Fig. 9. *Difference between soil surface temperature and room temperature with depth (1 inch = 2.54 cm)*

B. Pipe Cooling Cycle

There is a potential for a pipe transporting hot fluid to be located using IRT even after the pipe has been shut done, either for maintenance or to identify a problem. Thus determining how long it takes after the pipe has been shut down for the heat to dissipate and make the pipeline undetectable with IRT is important for inspection decision making. Cooling cycle for the 3" diameter CFRP pipe was monitored after pumping of hot water through it was stopped.

Soil surface temperature (IRT and TSC) had a sharper decrease during the first four days of cooling (from day 10 to 14) as illustrated in Fig. 10, with almost uniform daily room/ambient temperature. From the fourth to the eighth day (day 14 to 18), soil surface temperature remained constant with slight increase in ambient temperature, indicating a net decrease in soil temperature as shown in Fig. 11. Both the soil surface temperature and ambient temperature decreased between the eighth and eleventh days of cooling (day 18 to 21), indicating a net uniform soil temperature. A plot of the soil surface temperature difference is given in Fig. 11, showing a sharp temperature drop during first four days, a gently drop for the next four days of cooling, after which the soil temperature became almost constant/achieved steady state. Similar to the heating cycle, regular fluctuations in Fig. 10 and Fig. 11 are due to diurnal temperature changes.

The results in Fig. 10 and Fig. 11 indicate that, the same 7.6 cm (3") CFRP pipe in the same environmental conditions will be detectable using IRT up to the first eight days after pumping of hot fluid has been stopped. The heat will dissipate into the surrounding soil and the system will achieve a steady state after about eight days, and the pipe will not be detectable using IRT. Additional plots from the laboratory IRT test, including variations in pipe inlet and outlet temperatures, variations in pipe top and bottom temperatures, and soil temperature changes are available [9].

Table 1. *Field IRT test pipe parameters*

Depth, d (*cm*)	Depth, d (*in.*)	ΔT (°C)	TSC (°C)	Amb (°C)	TSC-Amb (°C)	IRT (°C)	IRT-Amb (°C)
30.5	12.00	47.2	38.3	21.5	16.8	40.8	19.3
35.6	14.00	55.1	30.4	21.5	8.9	32.9	11.4
40.6	16.00	62.9	22.5	21.5	1.0	25.0	3.5
42.0	16.50	64.9	21.5	21.5	0.0	23.1	1.6
42.5	16.75	65.9	21.5	21.5	0.0	22.1	0.6
43.2	17.00	66.9	21.5	21.5	0.0	21.5	0.0
45.7	18.00	70.8	21.5	21.5	0.0	21.5	0.0

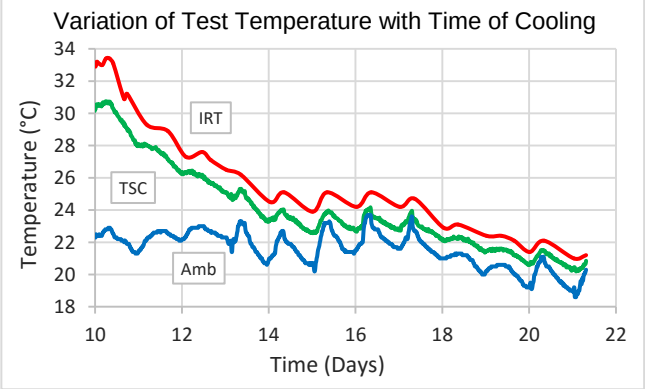

Fig. 10. *Variation of soil surface (TSC, IRT) and room (Amb) temperatures during cooling*

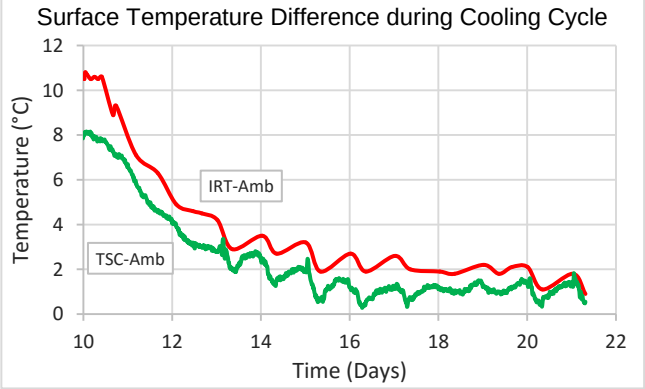

Fig. 11. *Soil surface temperature difference with time during cooling*

V. Testing of Field Pipes

After investigating the potential for IRT detection of buried pipe transporting hot water in the laboratory, testing of buried pipe operating in the field and transporting steam was carried out to study how the technique performs in the field environment. The field pipe is located at West Virginia University (WVU) campus and is used for transporting high pressure steam for on-campus heating. The pipe system consists of a 15.2 cm (6") diameter high pressure steam (HPS) line and a 7.6 cm (3") diameter condensate pumped (CP) line buried side-by-side in the same trench. The pipes had a minimum of 15.2 cm (6") poured in insulation around them (10.2 cm or 4" mineral fiber insulation at bends and expansion loops, and additional 15.2 cm or 6" poured in insulation through the entire pipe length). Details of the piping system are shown in Table 2 and Fig. 12.

Table 2. *Field IRT test pipe parameters*

Parameter	Value
Type of fluid	Steam, Condensate
Fluid temperature	105 °C (221 °F)
Pipe depth	76.2 – 91.4 cm (2.5' – 3')
Pipe diameter	6" and 3" (HPS and CP)
Pipe material	Steel
Pipe wall thickness	0.280" and 0.300" (HPS, CP)
Pipe insulation	6" min. insulation around pipes
Number of pipes	2: 6" and 3" diameters

IRT testing on the buried steam pipe was carried out in three different weather conditions (tests were done in winter, spring, and summer seasons). Results from these tests are summarized in Fig. 13 through Fig. 16. Fig. 13 shows a comparison between a visible image and IRT image taken at the site, with the identified features labelled. Fig. 14 shows IRT images of the pipe taken from a distance of about 1524 cm (50 ft.) from the pipe location in different weather conditions. For all IRT images in Fig. 14, the buried pipe is the first horizontal linear feature from the bottom of the image (first horizontal hot path from the bottom) as illustrated in Fig. 13. The buried pipe was easily detected using IRT in all weather conditions as shown in Fig. 14.

During IRT testing in winter, the ground was covered with snow up to a depth of 9.5 cm (3.75"). The snow cover however did not hinder the performance of this technique for buried pipe detection since the buried hot pipe increased temperature of the snow over the pipe to around 0.5°C compared to the surrounding snow-covered soil which had a temperature of -8.7°C as shown in Fig. 14(c). Soil surface temperature over the pipe during summer testing was measured to be 39°C, while temperature of the surrounding soil was measured to be 26°C. Fig. 15 shows IRT image of the pipe taken from close distance (about 152 cm or 5 ft. from the pipe) in different weather conditions. Plots of temperature distribution across the buried pipe (from the bottom to the top of each IRT scan in Fig. 15) in each season are shown in Fig. 16. It can be observed from Fig. 16 that, the buried hot pipe increased the soil surface temperature by 9.5°C to 20°C compared to the surrounding soil, thereby making it possible to detect this buried insulated pipe transporting high pressure steam.

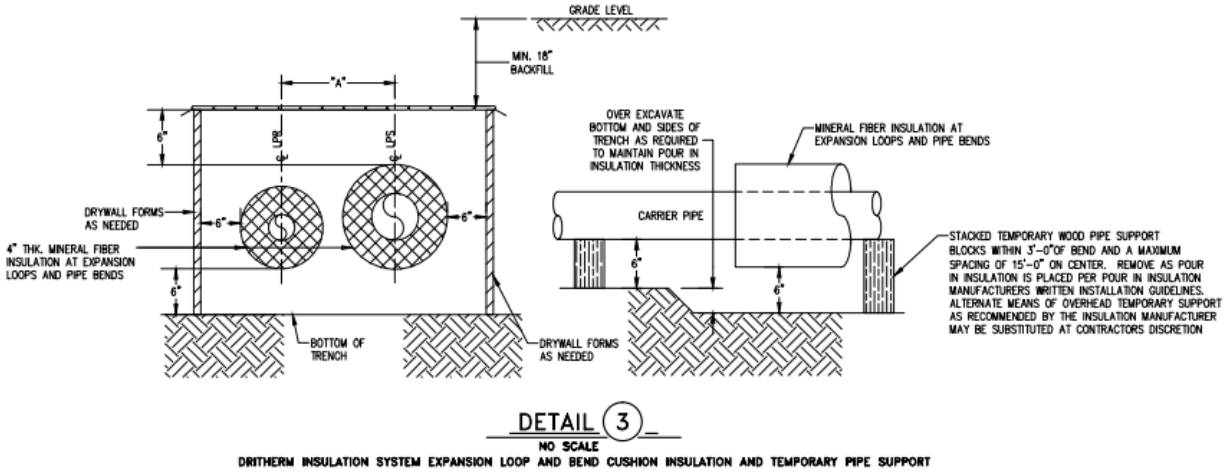

Fig. 12. *Field IRT test pipe installation details (Source: WVU Facilities Management)*

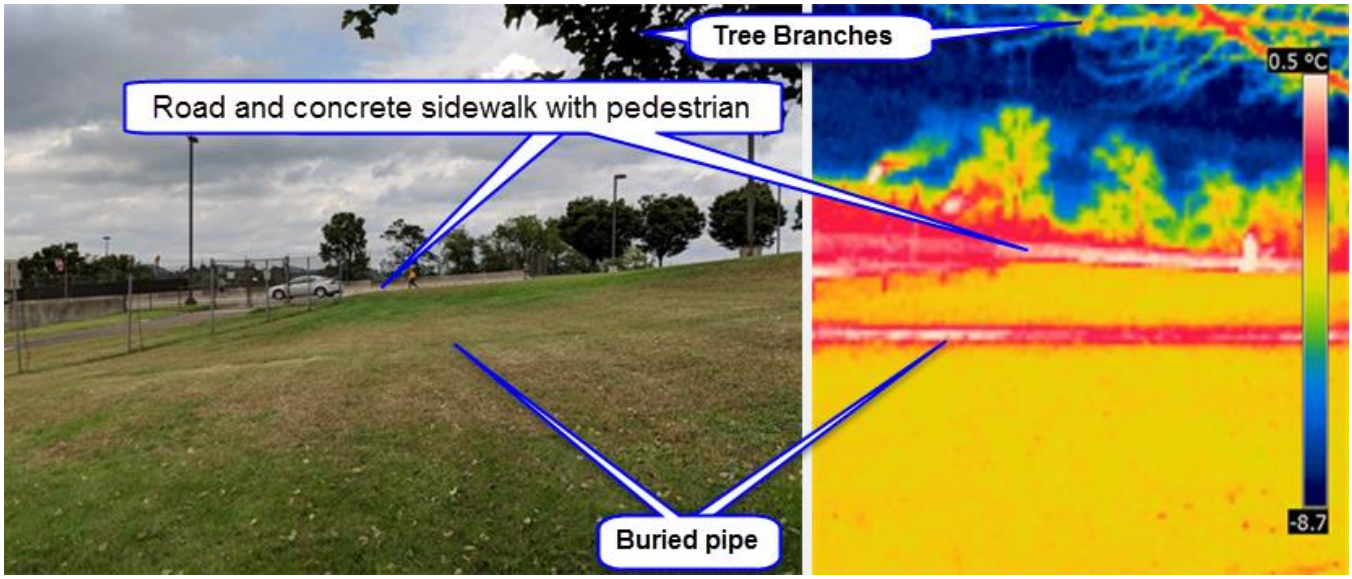

Fig. 13. *Comparison between IRT and visible image results*

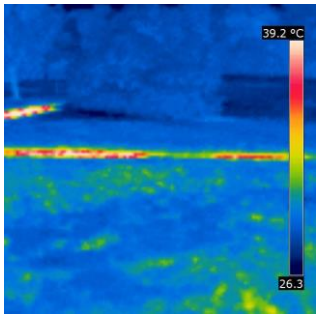

(a) Summer test result

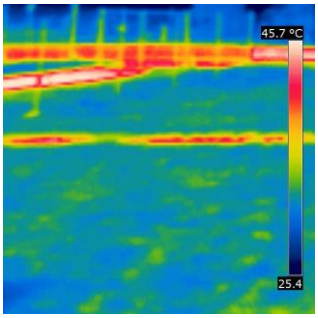

(b) Summer test from another angle

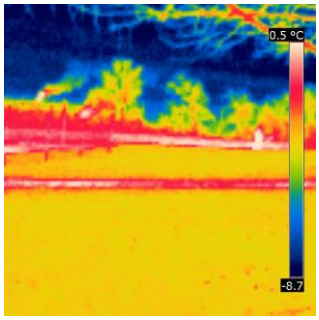

(c) Winter test result

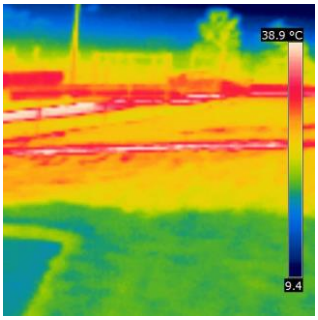

(d) Spring test result

Fig. 14. *Infrared thermography data at the soil surface in different seasons*

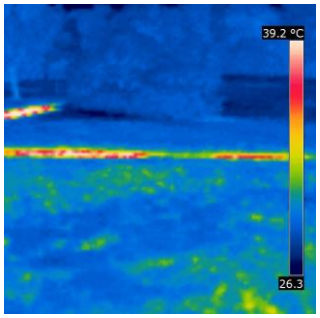

(a) Summer (longer distance)

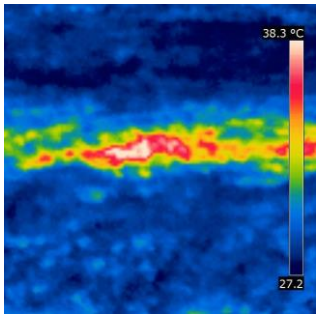

(b) Summer test result

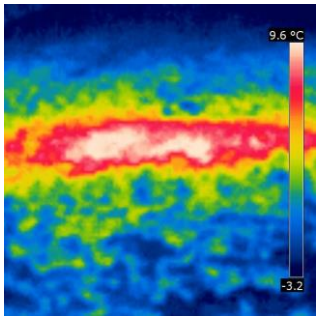

(c) Winter test result

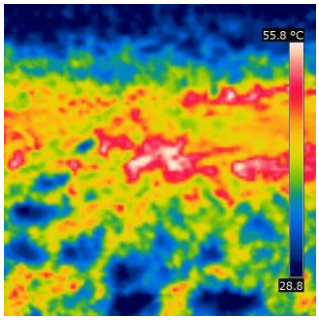

(d) Spring test result

Fig. 15. *Infrared thermography data at the soil surface taken from close range in different seasons*

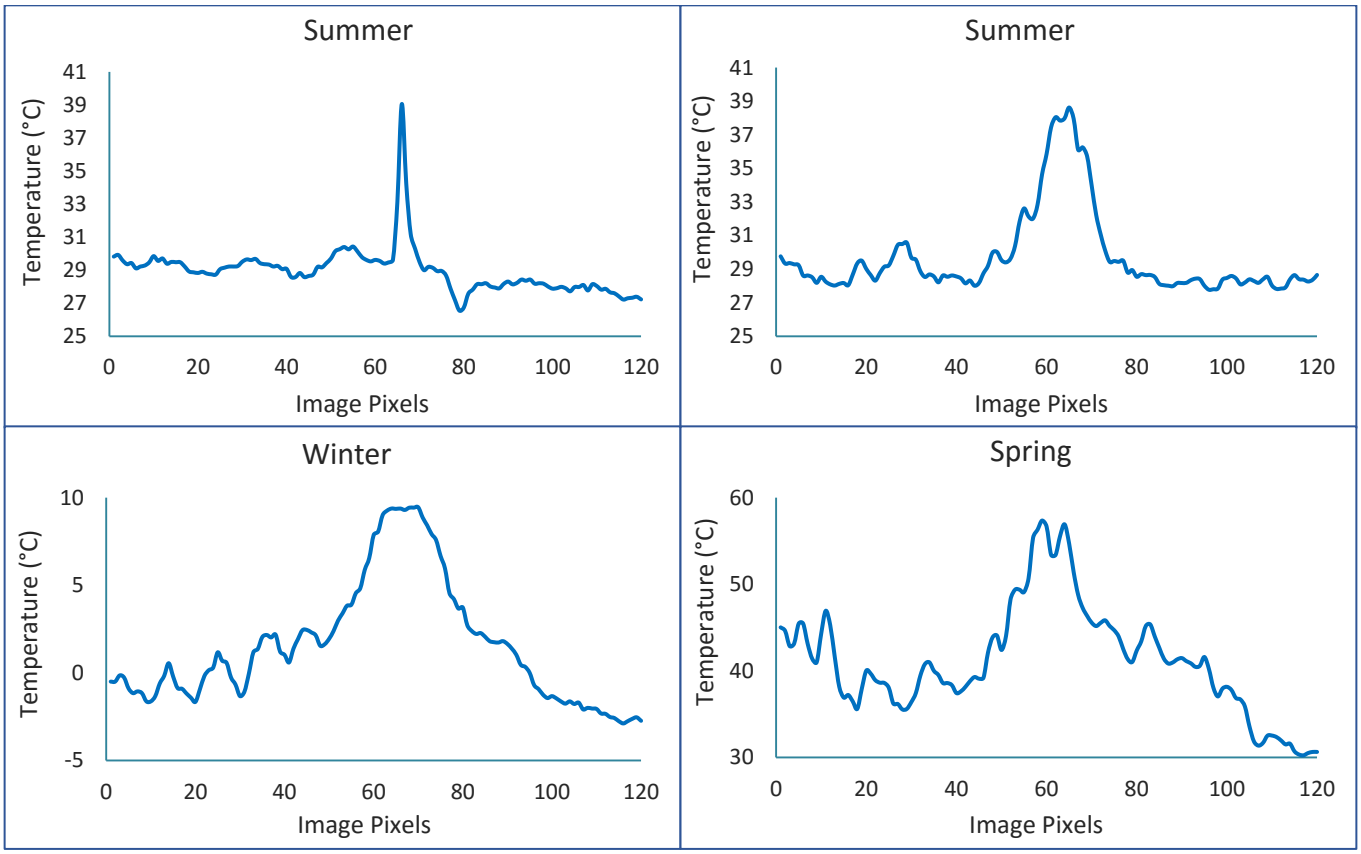

Fig. 16. *Temperature distribution across each IRT data in Fig. 15*

VI. Conclusions

The IRT test conducted in this research demonstrate that buried pipe transporting hot fluid such as steam or petroleum products from production wells or refinery plants have the potential of being detectable using IRT. The results from laboratory tests show that, IRT can be used to detect the 7.6 cm (3") CFRP composite pipe up to a depth of 42 cm (16.5") in the test medium when 95°C water is pumped through the pipe.

Test conducted on a buried pipe operating in the real world and transporting steam showed that, the IRT technique for detecting buried pipes transporting hot fluids has a better performance than the laboratory test suggested. Though the field pipe was buried at a much deeper depth of 76.2 – 91.4 cm (2.5' – 3') and was insulated to prevent loss of heat to the surrounding soil, the IRT technique performed remarkably well. This can be attributed to higher moisture content of the soil and higher compaction of the backfill material (leading to higher thermal conductivity) in the field compared to the laboratory work. The performance of the IRT technique is expected to be even better for pipes with less or no insulation at all (compared to the field pipe tested in this study). Performance of the IRT technique is also expected to be better for bigger diameter pipes.

Computations on the laboratory test data assumed a one-dimensional heat conduction equation to arrive at the depth of possible pipe detection. Heat transfer in the field environment will not be one-dimensional, but rather three-dimensional. Also, bigger diameter pipes (much bigger than 7.6 cm or 3") are used in the field to transport petroleum products at temperatures less than or equal to 200°F (93°C). This temperature is about equal to what was used in the laboratory test (water temperature was 95°C, but trapped air pocket above the water in the pipe reduced the pipe surface temperature at the top of the pipe by 4.5°C compared to the pipe surface temperature at the bottom of the pipe). The three-dimensional heat transfer in the field environment will reduce the depth of pipe detection to an extent, but the use of bigger diameter pipes, coupled with higher moisture content and better compaction of backfill material is expected to have a bigger effect in increasing the depth of possible detection using IRT.

Thus, IRT has the potential of being used in detecting pipelines transporting hot fluids, but the maximum depth at which the pipe can be detected will depend on the diameter of the pipe and the temperature of liquid being transported.

Acknowledgment

The authors gratefully acknowledge the financial support provided by the United States Department of Transportation - Pipeline and Hazardous Materials Safety Administration (USDOT-PHMSA) through the Competitive Academic Agreement Program (Project # DTPH5615HCAP09).

The authors would also like to thank Mr. Jerry Nestor, Lab Instrumentation Specialist at West Virginia University, Constructed Facilities Center (WVU-CFC) for his help in building the wooden box and pipe setup for laboratory IRT testing.

REFERENCES

[1] Sakagami, T., Izumi, Y., Kobayashi, Y., Mizokami, Y., & Kawabata, S. “Applications of infrared thermography for nondestructive testing of fatigue cracks in steel bridges,” in Thermosense: Thermal Infrared Applications XXXVI, Fred P. Colbert and Sheng-Jen (Tony) Hsieh, Eds. Proceedings of SPIE Vol. 9105, 91050S, 2014.

[2] Mitani, K., & Matsumoto, M. “Innovative bridge assessment methods using image processing and infrared thermography technology,” Proceedings of the 37th Conference on Our World in Concrete & Structures, Singapore. 2012

[3] Taillade, F., Quiertant, M., Benzarti, K., Dumoulin, J., & Aubagnac, C. “nondestructive evaluation of FRP strengthening systems bonded on RC structures using pulsed stimulated infrared thermography,” in Infrared Thermography, R. V. Prakash, Ed. InTech, 2012.

[4] Ghosh, K. K., & Karbhari, V. M. “Use of infrared thermography for quantitative non-destructive evaluation in FRP strengthened bridge systems,” Materials and Structures, 44(1), 169-185, 2011.

[5] Spring, R., Huff, R., & Schwoegler, M. “Infrared thermography: a versatile nondestructive testing technique,” Materials Evaluation, 69(8), 934-942, 2011.

[6] Halabe, U. B., & Dutta, S. S. “Quantitative characterization of debond size in FRP wrapped concrete cylindrical columns using infrared thermography,” The Fourth Japan-US Symposium on Emerging NDE Capabilities for a Safer World, Makena Beach & Resort Hotel, Maui Island, Hawaii, USA, 2010.

[7] Halabe, U. B., Dutta, S. S., and GangaRao, H. V. S., “Infrared thermographic and radar testing of polymer-wrapped composites,” Materials Evaluation, Vol. 68, No. 4, April, 2010, pp. 447-451.

[8] Halabe, U. B., Vasudevan, A., Klinkhachorn, P., and GangaRao, H. V. S., “Detection of subsurface defects in fiber reinforced polymer composite bridge decks using digital infrared thermography,” Nondestructive Testing and Evaluation, Vol. 22, Nos. 2-3, June-September, 2007, pp. 155-175.

[9] Kavi, J., “Detection of Buried Non-Metallic (Plastic and FRP Composite) Pipes Using GPR and IRT," Ph.D. Dissertation, Department of Civil and Environmental Engineering, West Virginia University, Morgantown, WV, USA, December, 2018.